Electronic Supplementary Information (ESI) for

Nanostructured nickel/carbon matrix as efficient oxygen evolution reaction electrocatalyst for rechargeable zinc-air batteries

Chengqiang Cui,[a,1] Xiaoming Ge,[b,1] Tao An,[b] Bing Li,[b] Delvin Wuu,[b] Nguk Neng Tham,[b] Kai Zhang,[a] Yunbo He,[*a] and Zhaolin Liu[*b]

[a] School of Electromechanical Engineering, Guangdong University of Technology, No. 100 Waihuan Xi Road, Guangzhou 510006, China. Email: heyunbo@gdut.edu.cn

[b] Institute of Materials Research and Engineering (IMRE), A*STAR (Agency for Science, Technology and Research), 2 Fusionopolis Way, Innovis, #08-03, Singapore 138634, Republic of Singapore. Email: zl-liu@imre.a-star.edu.sg

1: These authors contributed equally.

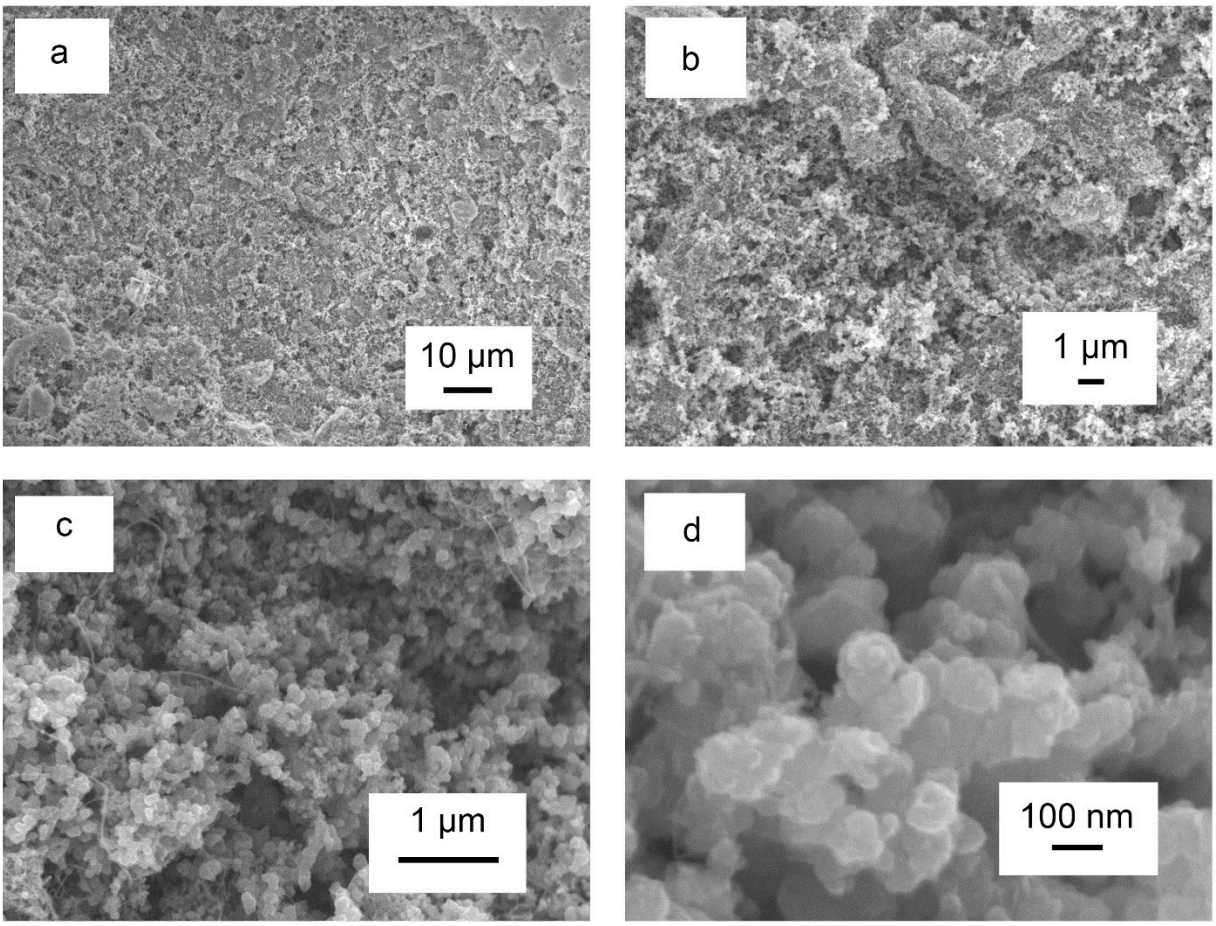

Figure S1. Scanning electron microscopy (SEM) surface morphology images of 10 BN GDL carbon paper at different magnifications.

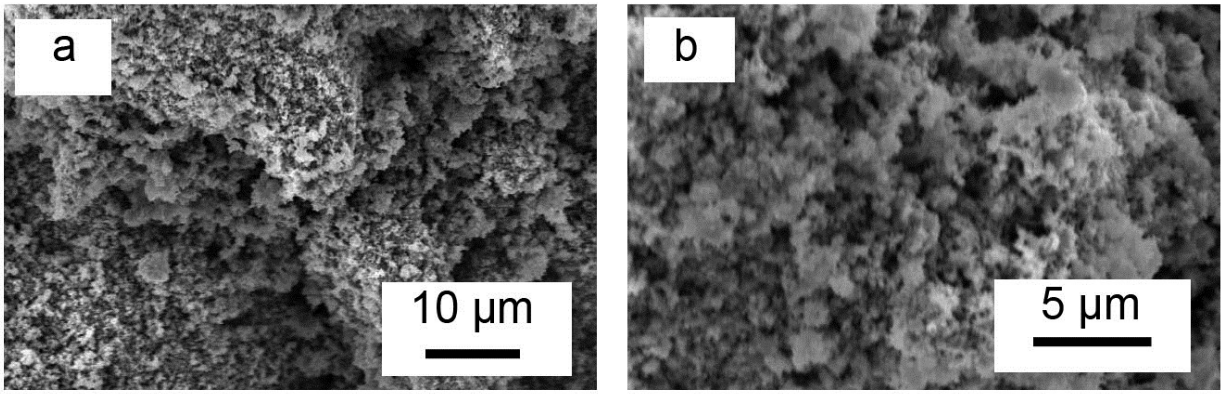

Figure S2. SEM surface morphology images of Ni/2MI precursor grown on 10 BN GDL carbon paper at the magnification of ×2000 (a) and ×5000 (b).

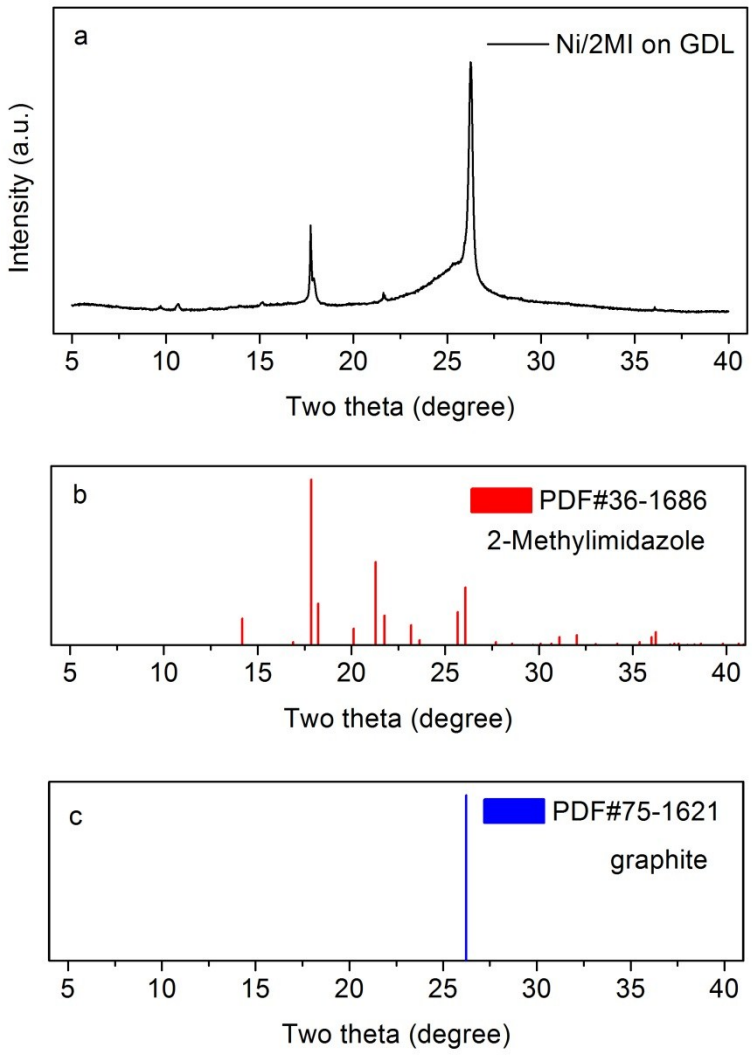

Figure S3. (a) X-ray diffraction (XRD) pattern of Ni/2-methylimidazolate (Ni/2MI) grown on 10 BN GDL carbon paper. (b) Powder diffraction file (PDF) No. 36-1686 which is 2-methylimidazole. (c) PDF No. 75-1621 which is graphite. Note that no Ni species is observed in (a) because of the detection limit of XRD.

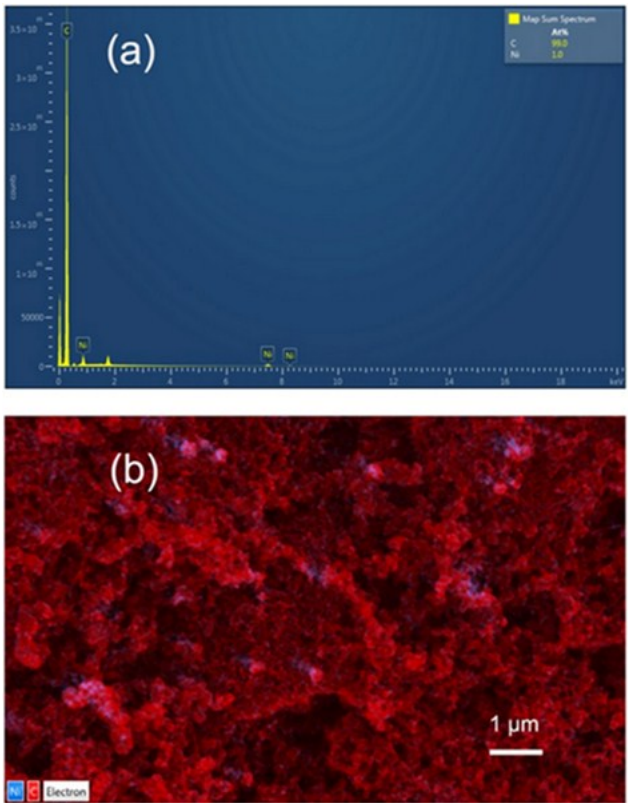

Figure S4. (a) EDX spectrum and (b) EDX mapping of a Ni/C oxygen evolution electrode.

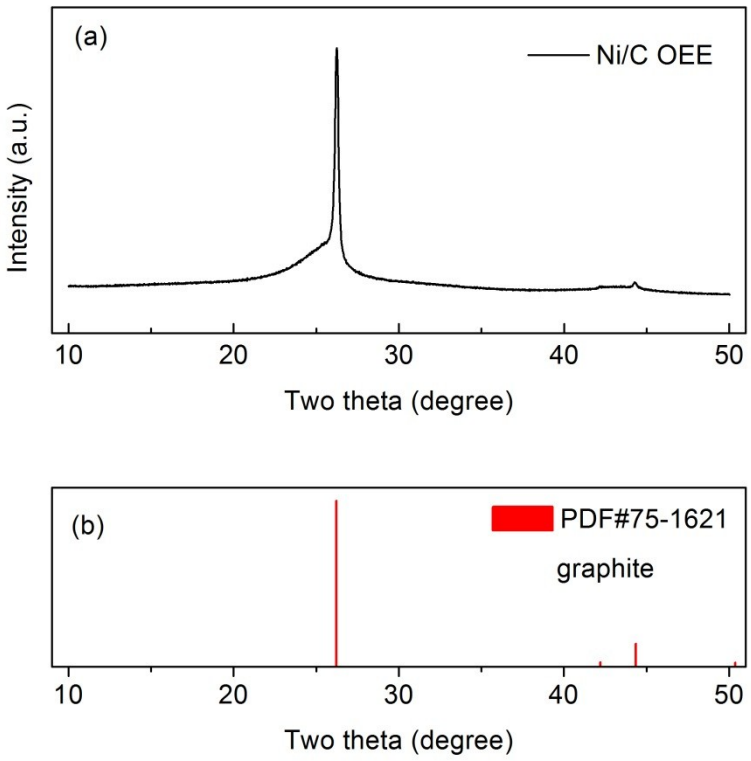

Figure S5. (a) XRD pattern of Ni/C oxygen evolution electrode (OEE). (b) PDF No. 75-1621 which is graphite. Note that no Ni species is observed because of the detection limit of XRD.

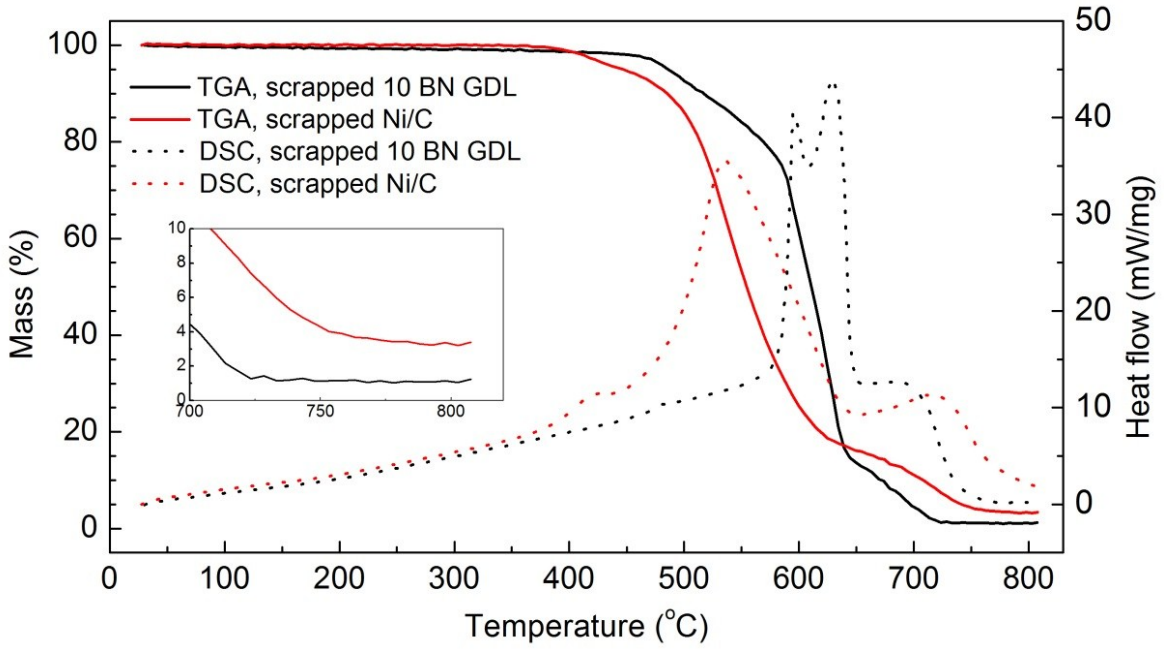

Figure S6. TGA/DSC profiles of Ni/C powders and carbon powders scrapped from the surface of Ni/C OEE and blank GDL carbon paper, respectively. TGA/DSC profiles show that the Ni/C OEE has 3.37 wt.% of solid ashes, comprising 2.22 wt.% of NiO and 1.15 wt.% of intrinsic ashes of blank GDL. The 2.22 wt.% NiO is equivalent to 0.36 at.% of Ni species in the scrapped Ni/C powders (*cf.* 1 at.% Ni given by EDX, Figure 1a). It is conceivable for a lower Ni loading recorded by TGA/DSC than that by EDX, because carbon black powers on GDL carbon paper were scrapped off together with Ni/C catalysts during the sample collection.

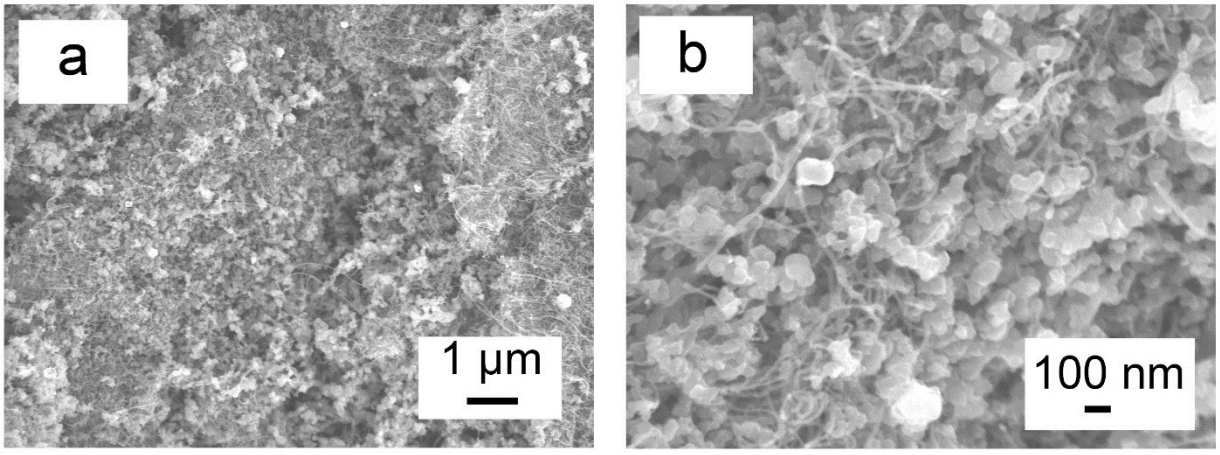

Figure S7. SEM surface morphology images of Ni/C OEE under magnification of ×10,000 (a) and ×50,000 (b).

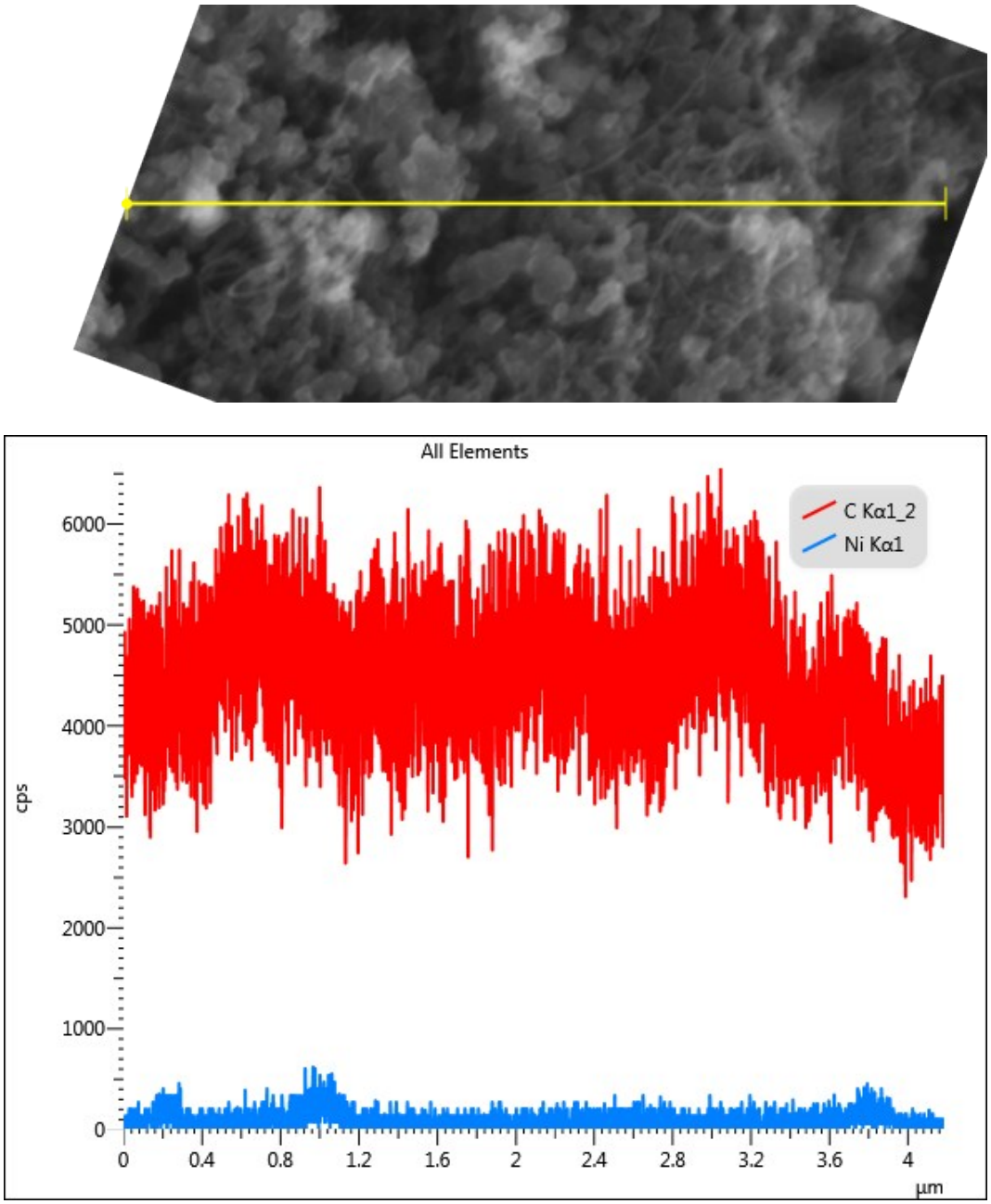

Figure S8. EDX line-profiling across the surface of Ni/C OEE. The spectrum (bottom) corresponds to the yellow line in the SEM image (top). The result indicates some Ni-rich regions around 0.2 µm, 0.9 µm and 3.8 µm in size.

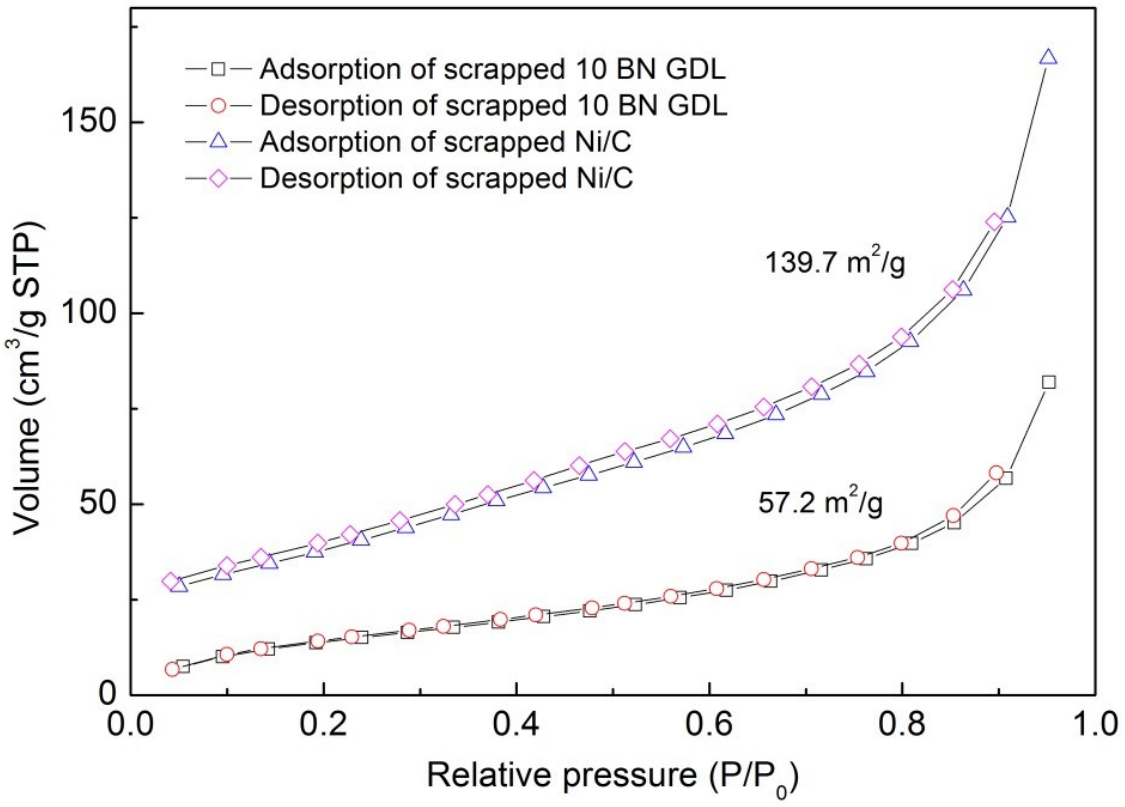

Figure S9. Nitrogen adsorption/desorption isotherms of powders scrapped from 10 BN GDL carbon paper and Ni/C OEE. The result shows 214% improvement of the BET surface area of 10 BN GDL carbon paper after the growth of Ni/C on its surfaces, demonstrating the porous nature of the Ni/2MI complex-derived carbon support.

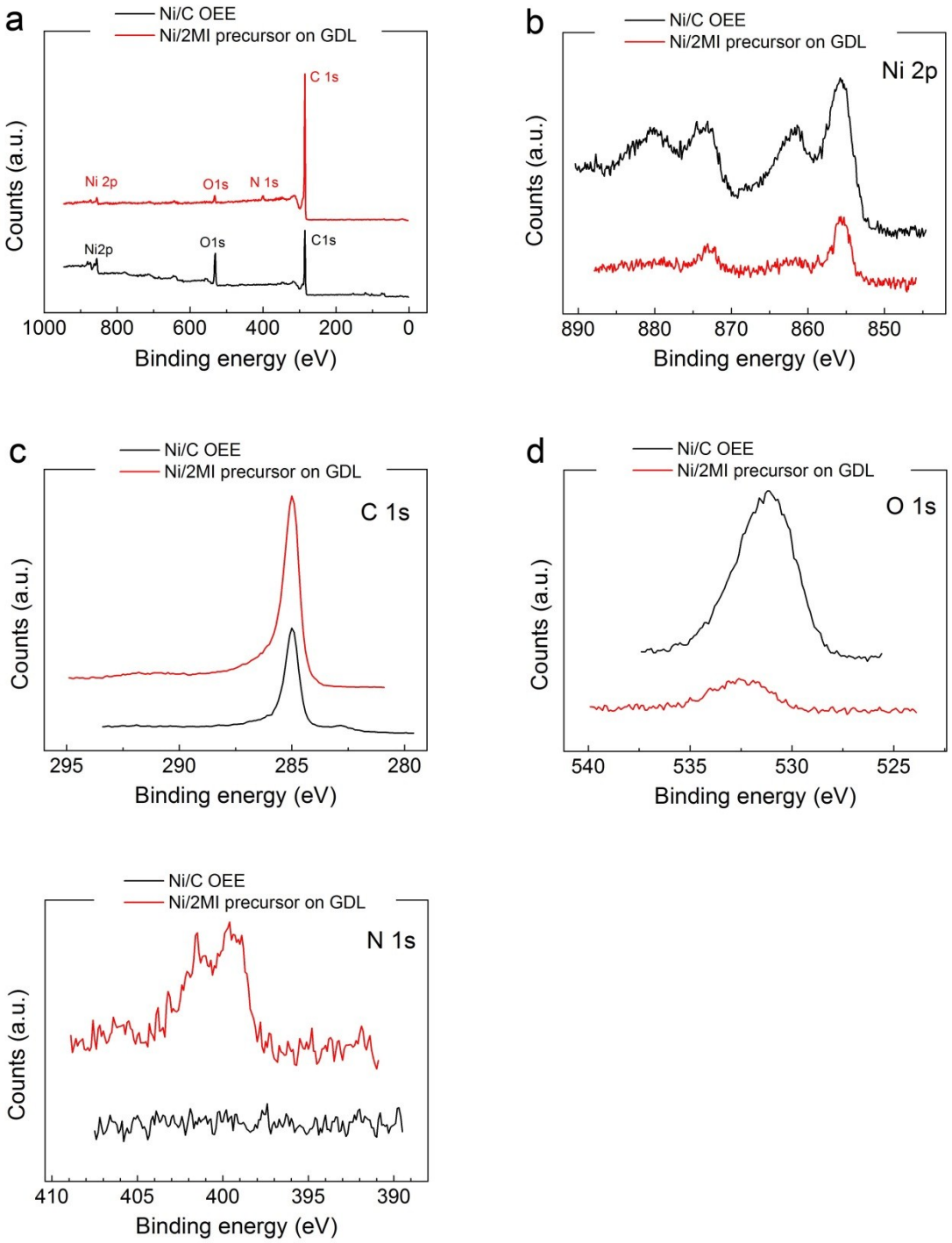

Figure S10. XPS spectra of Ni/2MI on GDL carbon paper and Ni/C oxygen evolution electrode: (a) survey scans, (b) Ni 2p, (c) C 1s, (d) O 1s and (e) N 1s.

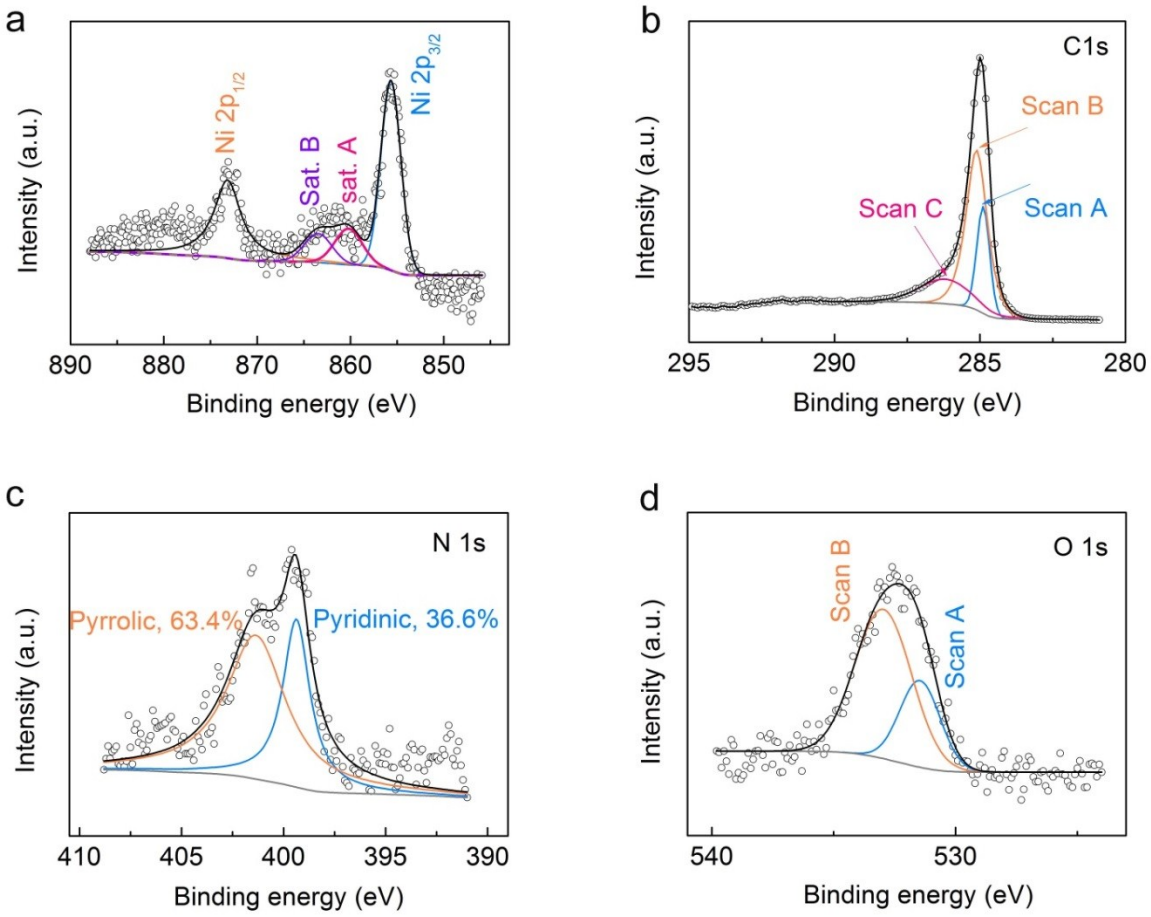

Figure S11. Fitted high-resolution XPS spectra of Ni/2MI on GDL carbon paper: (a) Ni 2p, (b) C 1s, (c) N 1s and (d) O 1s.

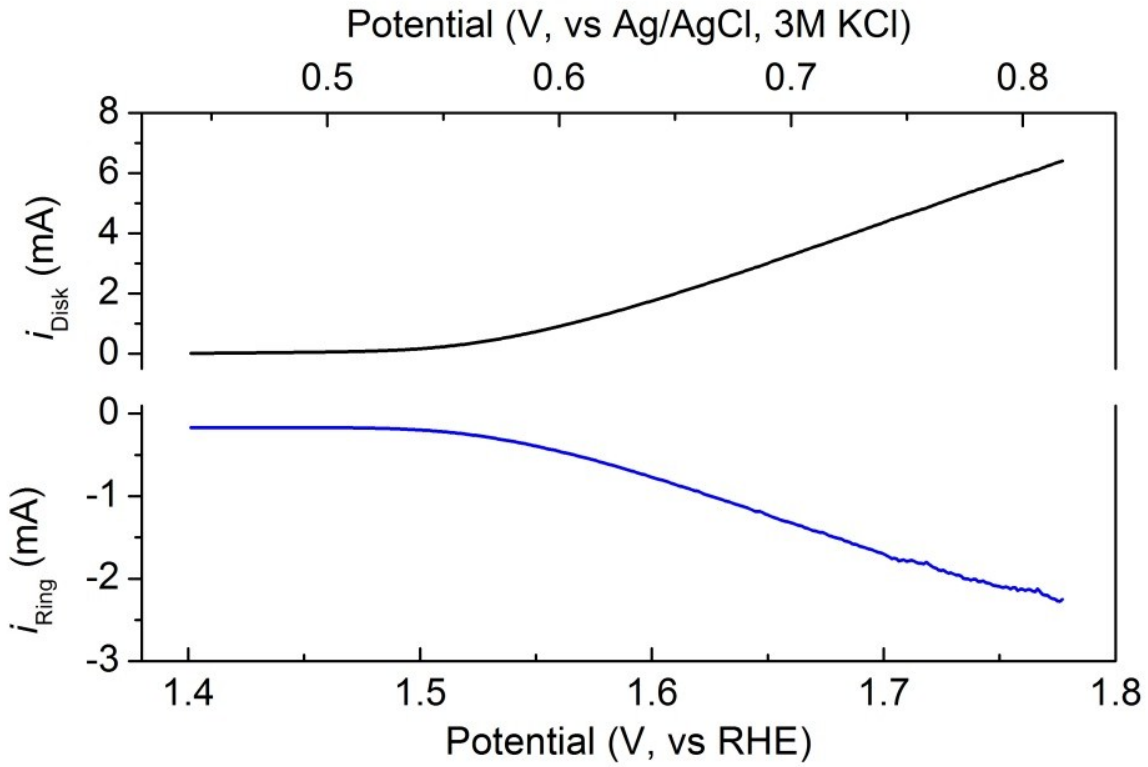

Figure S12. Disk ($4OH^- \rightarrow 2H_2O + O_2 + 4e^-$) and ring ($2H_2O + O_2 + 4e^- \rightarrow 4OH^-$) currents of RRDE loaded with 0.1 mg cm^{-2} scrapped Ni/C. The electrolyte is N_2-saturated 0.1 M KOH. The rotating rate of RRDE is 1600 rpm. The sweeping rate is 10 mV s^{-1}. The collection efficiency of RRDE obtained from E_{ring} = 1.60 V to 1.75 V is (39.2 ± 1.8) %, close to manufacturer's data of 37% (www.pineinst.com).

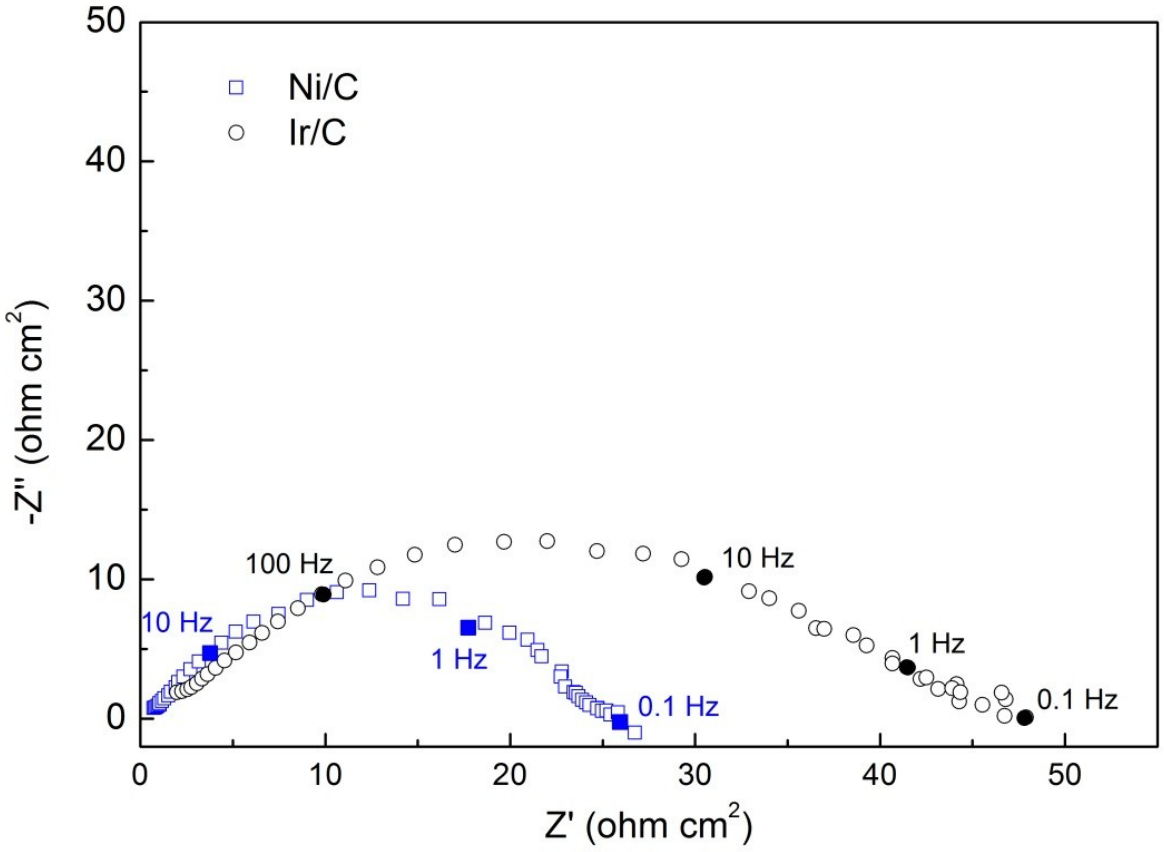

Figure S13. Impedance spectra of Ir/C and Ni/C RDE under a rotating rate of 400 rpm. The working electrode is polarized at 1.61 V. Ni/C catalysts are scrapped from a Ni/C OEE. The electrolyte is O_2-saturated 0.1 M KOH solution.

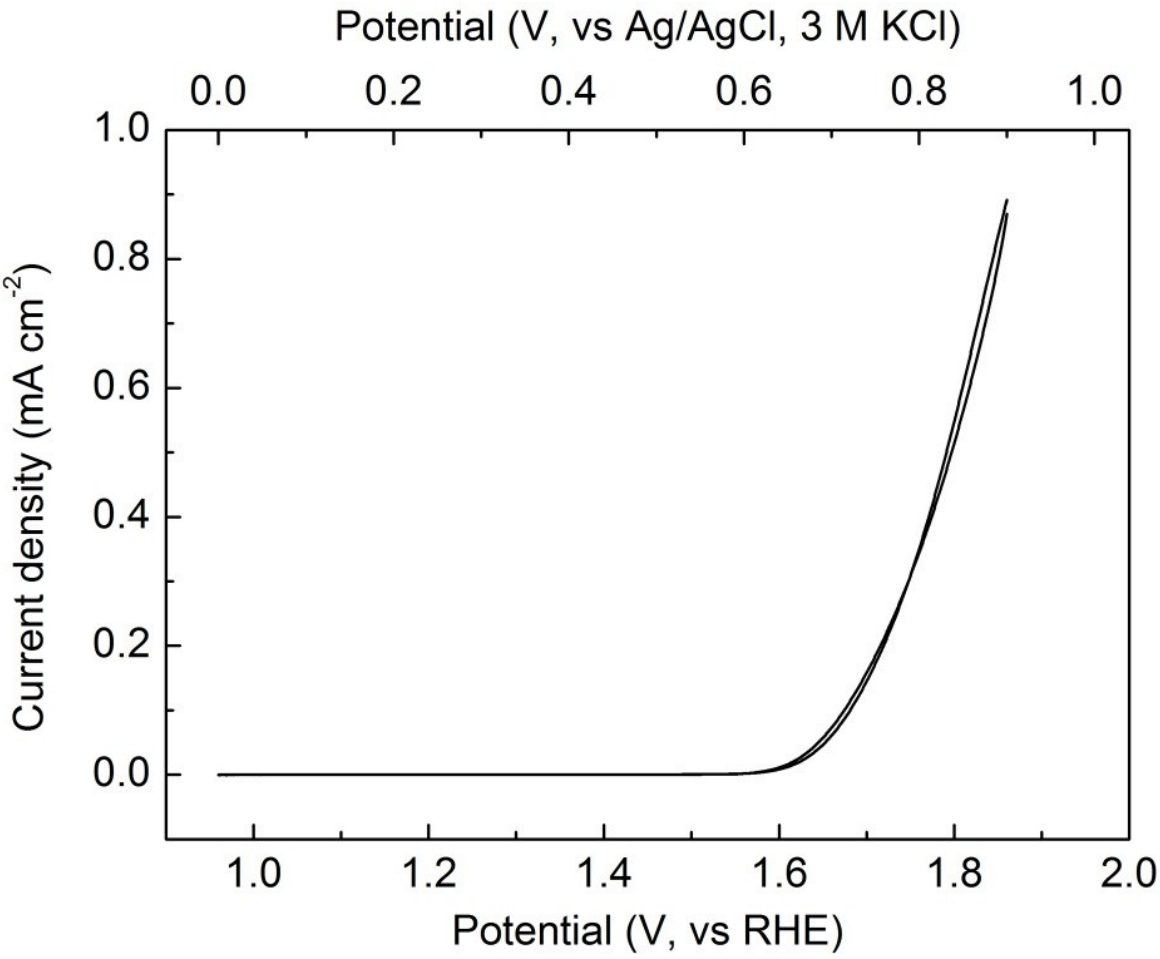

Figure S14. Cyclic voltammogram of blank GDL in O_2-saturated 0.1 M KOH solution.

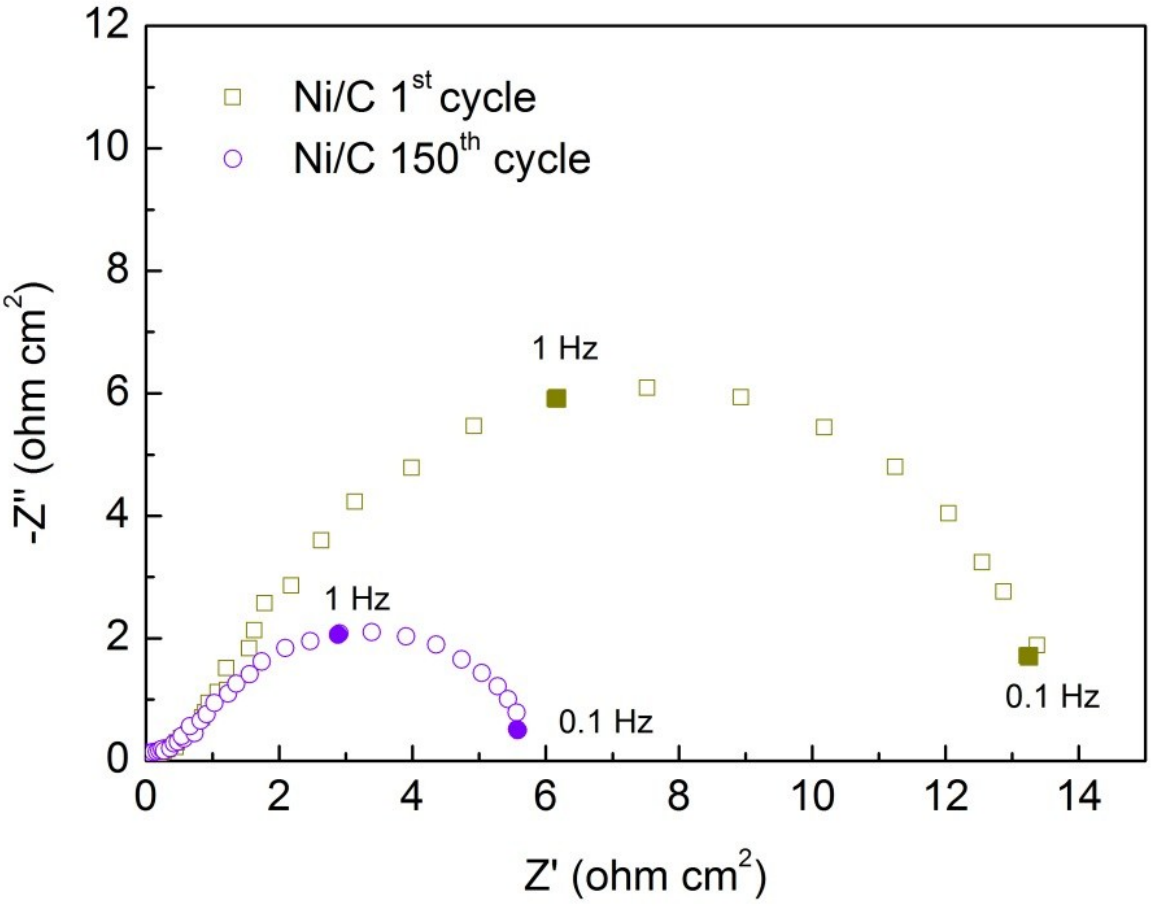

Figure S15. Impedance spectra of Ni/C OEE which is subjected to cyclic voltammetric degradation tests from 1.04 V to 1.88 V. The electrolyte is O_2-saturated 0.1 M KOH solution.

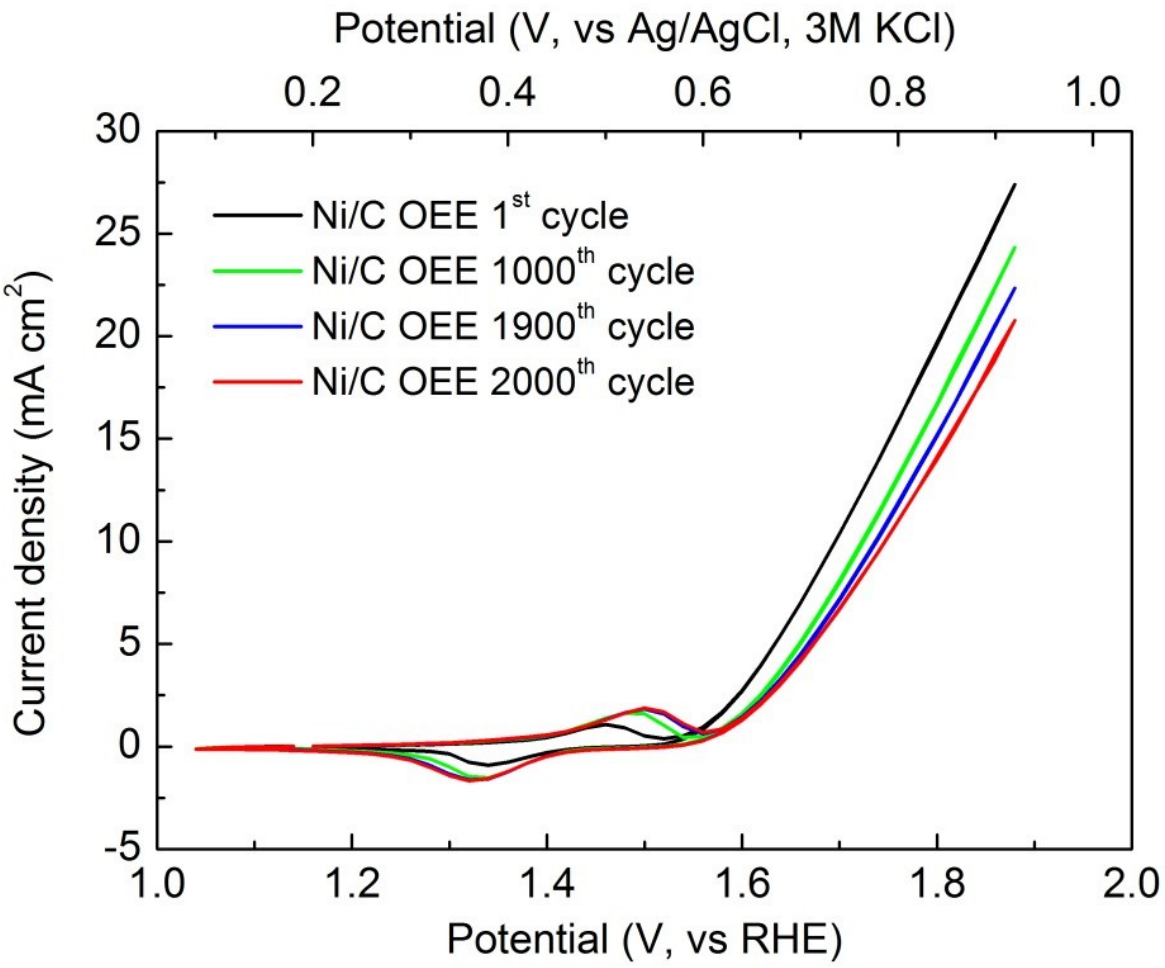

Figure S16. Cyclic voltammograms of Ni/C OEE in O_2-saturated 0.1 M KOH solution.

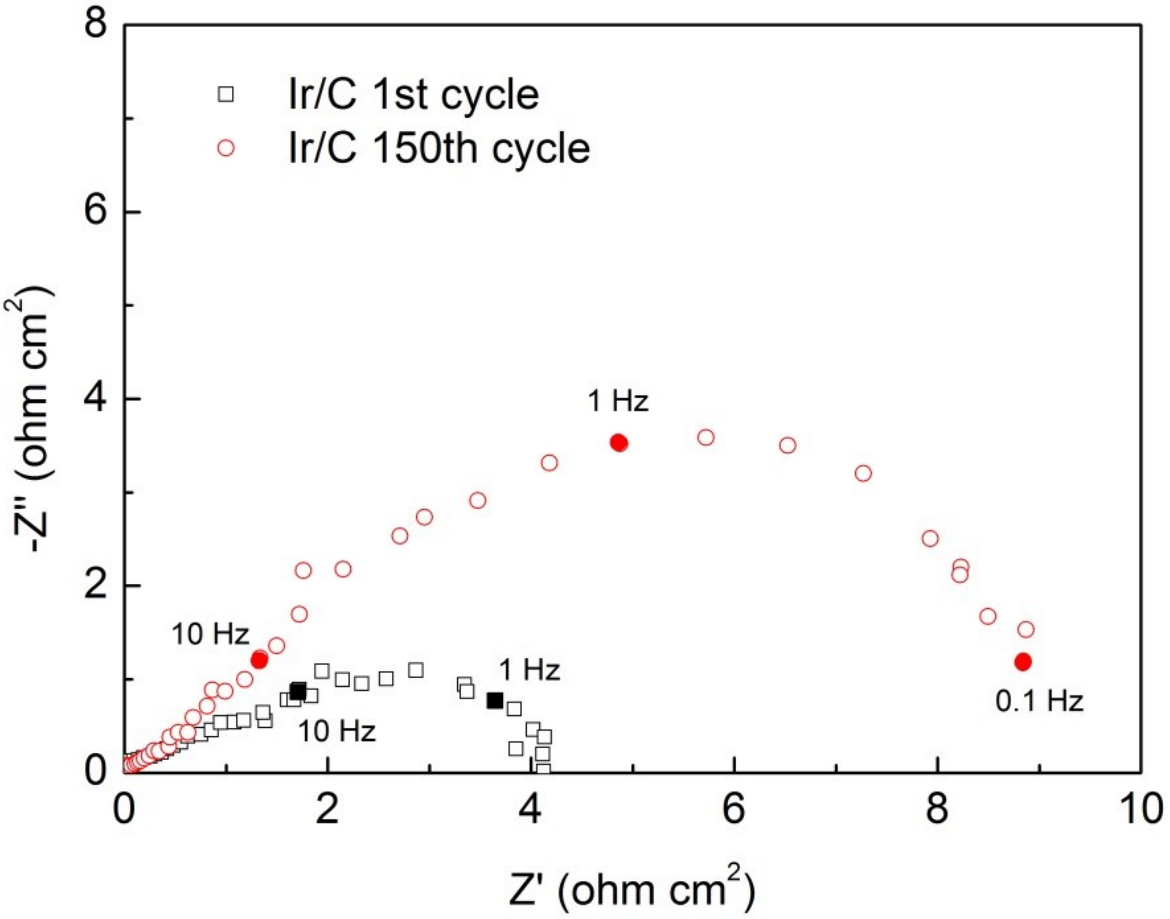

Figure S17. Impedance spectra of Ir/C OEE which is subjected to cyclic voltammetric degradation tests from 1.04 V to 1.88 V. The electrolyte is O_2-saturated 0.1 M KOH solution.

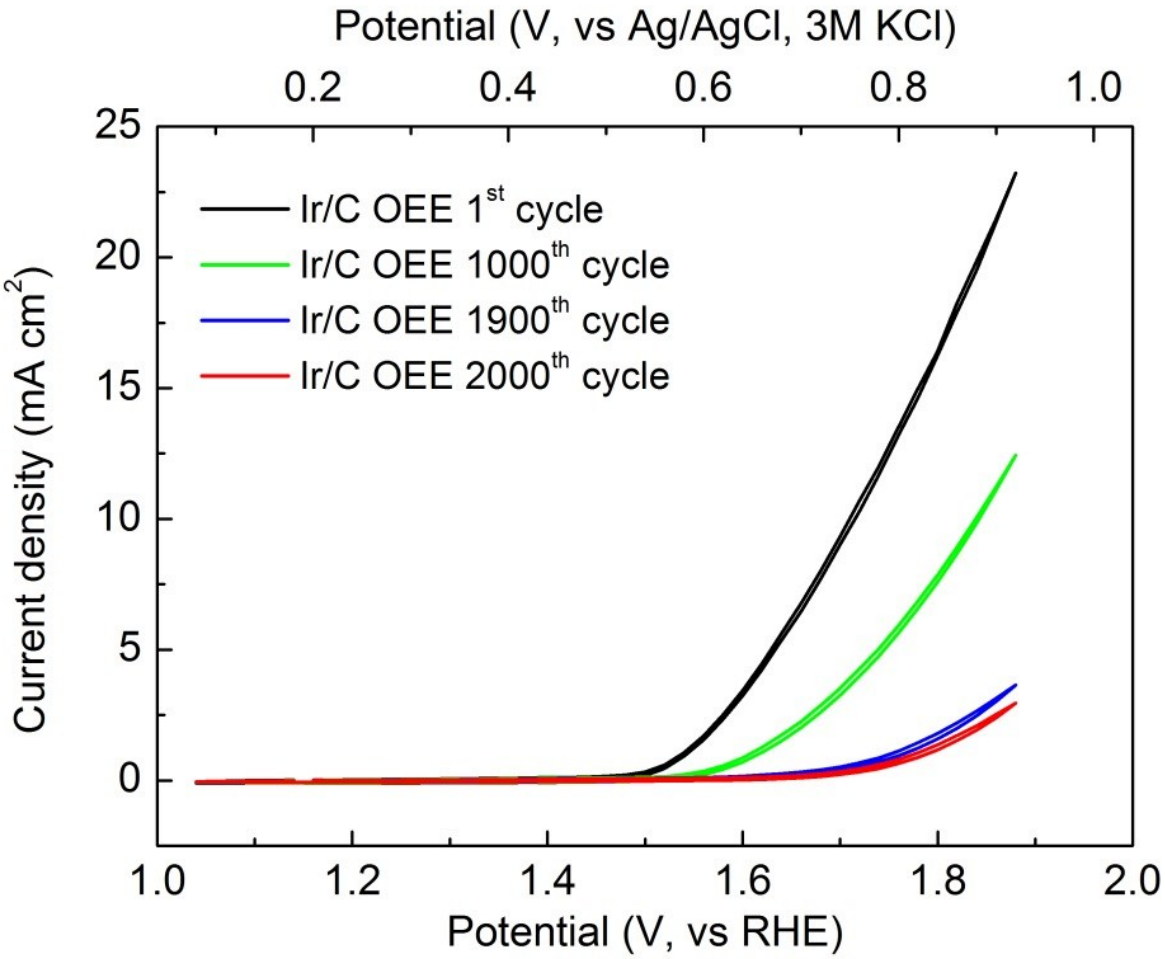

Figure S18. Cyclic voltammograms of Ir/C OEE in O_2-saturated 0.1 M KOH solution.

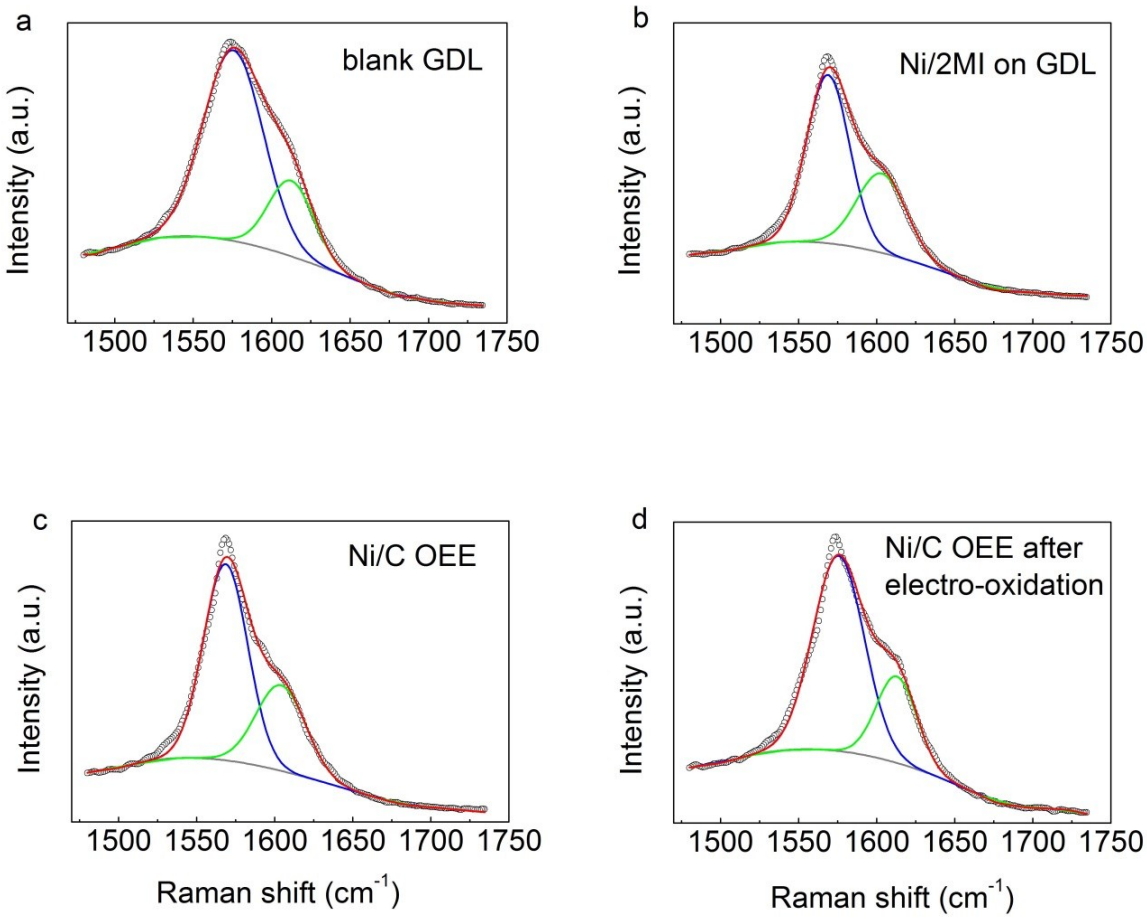

Figure S19. Fitted carbon G band Raman spectra of blank GDL carbon paper (a), Ni/2MI on GDL carbon paper (b), Ni/C OEE (c) and Ni/C OEE after electro-oxidation (d): experimental (black open dot), envelope (red line), main peak (blue line), shoulder peak (green line), and background (gray line). The fitting procedure is based on Gaussian peaks (Origin Pro 8 Peak Analyzer package). The electro-oxidation was conducted by 3 cyclic voltammetric scans from 0.96 V to 1.76 V with a sweeping rate of 0.5 mV s^{-1}.

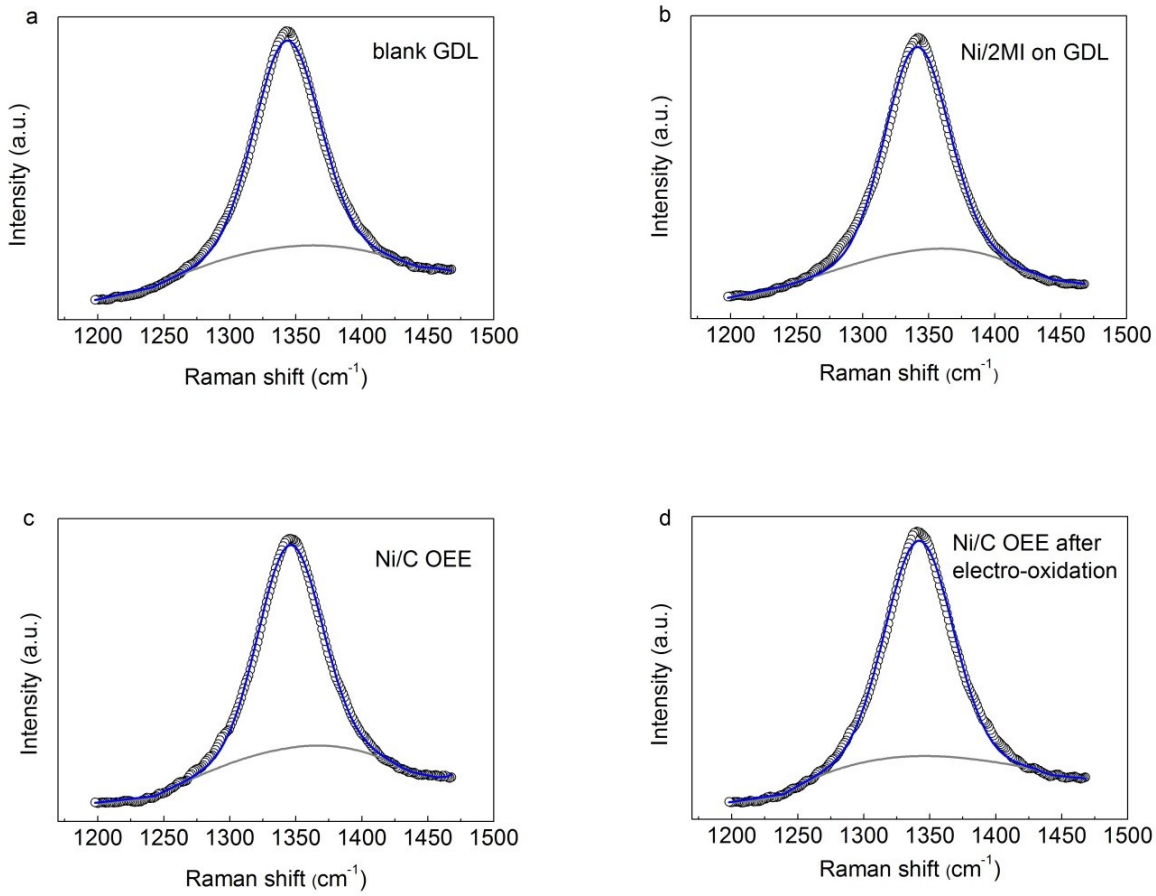

Figure S20. Fitted carbon D band Raman spectra of blank GDL carbon paper (a), Ni/2MI on GDL carbon paper (b), Ni/C OEE (c) and Ni/C OEE after electro-oxidation (d): experimental (black open dot), fitted peak (blue line), and background (gray line). The fitting procedure is based on Gaussian peaks (OriginPro 8 Peak Analyzer package). The electro-oxidation was conducted by 3 cyclic voltammetric scans from 0.96 V to 1.76 V with a sweeping rate of 0.5 mV s^{-1}.

Table S1. Fitted carbon G band of Raman spectra of blank GDL carbon paper, Ni/2MI on GDL carbon paper, Ni/C OEE, and Ni/C OEE after electro-oxidation.

	G band			D band	D band/ G band peak area ratio	D band/ G band main peak height ratio
	Center of main peak (cm^{-1})	Center of shoulder peak (cm^{-1})	Should/main peak area ratio	Peak center (cm^{-1})		
Blank GDL	1575.5	1612.5	0.30	1343.4	0.92	0.92
Ni/2MI on GDL	1568.8	1603.2	0.54	1341.1	0.95	0.85
Ni/C OEE	1568.5	1604.0	0.49	1341.9	0.88	0.73
Ni/C OEE after electro-oxidation	1575.5	1612.7	0.35	1345.7	0.82	0.76